

金属氯化物-苯并噻唑有机-无机杂化化合物的合成、表征及荧光性质

刘 庆 魏振宏* 于 慧 郝艳欢 蔡 琥*

(南昌大学化学学院, 南昌 330031)

摘要: 金属氯化物 MCl_2 ($M=Pb^{2+}, Cd^{2+}, Co^{2+}$) 分别与苯并噻唑(btz)在浓盐酸中、80 °C 下反应, 合成了 3 种有机-无机杂化化合物: $(btzH)[(PbCl_3)]$ (**1**), $(btzH)_2[CdCl_4] \cdot 2H_2O$ (**2**) 和 $(btzH)_2[CoCl_4] \cdot 2H_2O$ (**3**), 其中化合物 **2** 和 **3** 结构相似。对化合物 **1~3** 进行了粉末衍射、红外和紫外光谱、元素分析、热重分析以及 X 射线单晶衍射表征。荧光测试发现: 化合物 **1~3** 在 393 nm 处有发射峰, 该荧光来源于苯并噻唑环中电子的 $\pi \cdots \pi$ 跃迁。

关键词: 金属氯化物; 苯并噻唑; 有机-无机杂化; 晶体结构; 荧光性质

中图分类号: O614.43+3; O614.24+2; O614.81+2

文献标识码: A

文章编号: 1001-4861(2017)11-2139-08

DOI: 10.11862/CJIC.2017.258

Syntheses, Characterization and Optical Properties of Three Organic-Inorganic Hybrid Compounds Based on Metal Chlorides and Benzothiazole

LIU Qing WEI Zhen-Hong* YU Hui HAO Yan-Huan CAI Hu*

(College of Chemistry, Nanchang University, Nanchang 330031, China)

Abstract: The reaction of three divalent metal (II) halides MCl_2 ($M=Pb^{2+}, Cd^{2+}, Co^{2+}$) with two equivalents of benzothiazole (btz) in the concentrated acid HCl at 80 °C resulted in the formation of the corresponding organic-inorganic hybrid compounds: $(btzH)[(PbCl_3)]$ (**1**), $(btzH)_2[CdCl_4] \cdot 2H_2O$ (**2**) and $(btzH)_2[CoCl_4] \cdot 2H_2O$ (**3**), in which the structures of compounds **2** and **3** are similar. All compounds have been characterized by XRD, IR, UV-Vis, EA, TG and single X-ray diffraction. Fluorescent investigation reveals that compounds **1~3** exhibit similar emission peaks at 393 nm, which are ascribed to the $\pi \cdots \pi$ transition of the btz ring. CCDC: 1571943, **1**; 1571944, **2**; 1571945, **3**.

Keywords: metal chloride; benzothiazole; organic-inorganic hybrid; crystal structure; fluorescent property

0 Introduction

Organic-inorganic hybrid perovskite functional materials are a new type of crystal materials, in which the inorganic perovskite layer works as a skeleton and the organic molecular functional groups are connected to the inorganic perovskite layer through intermolecular hydrogen bonds^[1-4]. The organic and inorganic components form a long-range ordered single crystal

through the alternating stacking, in which the inorganic parts supply the hybrid structure with thermal stability and hardness as well as optical, electrical and magnetic properties^[5-8], and the organic materials offer the hybrids with softness, flexibility, and highly efficient luminescence^[9] and structural diversity^[10-13]. Over the past decade, organic-inorganic hybrid compounds have exhibited good development and application in the solar semiconductor batteries^[14],

收稿日期: 2017-09-09。收修稿日期: 2017-10-15。

国家自然科学基金(No.21571094, 21661021)和江西省科技厅项目(No.20161BAB203073)资助。

*通信联系人。E-mail: weizh@ncu.edu.cn, caihu@ncu.edu.cn

light-emitting diodes^[15], ferroelectric properties^[9] and other fields^[16-18].

In organic-inorganic hybrid materials, the organic ligands not only play a role as the template^[19-21], but also the key to determining the properties of inorganic components^[22-24], such as in photoelectric field, the organic-inorganic hybrids constructed with organic amines and lead halide have shown good fluorescence performance^[25-27]. This is because the hybrid perovskite is a type of semiconductor quantum well structure, typically with small band gap inorganic sheets (carrier) alternating with larger band gap organic layer^[28-30]. For example, the new reported 2D lead bromide perovskite (DMEN)PbBr₄ (DMEN = 2-(dimethylamino) ethylamine) incorporating a bifunctional ammonium dication as template was found to have white-light, broad-band emission in the visible range^[25].

In this article, an aromatic heterocycle organic template benzothiazole (btz) was selected to react with the main and transition metal halides MCl₂ (M = Pb²⁺, Cd²⁺, Co²⁺) in the concentrated HCl acid, and three inorganic-organic hybrid compounds: (btzH)[PbCl₃] (**1**), (btzH)₂[CdCl₄]·2H₂O (**2**) and (btzH)₂[CoCl₄]·2H₂O (**3**) were obtained. Herein, we reported the syntheses, characterizations and fluorescent properties of compounds **1**, **2** and **3**.

1 Experimental

1.1 Instrument and materials

The starting materials PbCl₂, CdCl₂, CoCl₂·6H₂O, benzothiazole and the concentrated hydrochloric acid are commercially available and were used as received. FT-IR spectra were recorded using KBr pellets in the range of 4 000~400 cm⁻¹ on an ALPHA spectrometer. UV-Vis spectra were collected on a UV-Vis Curry 60 spectrophotometer. Powder X-ray diffraction (PXRD) patterns were collected on a glass sheet in the 2θ range of 5°~50° with a scan rate of 2°·min⁻¹ on a D8 ADVANCE diffractometer equipped with Cu Kα radiation (λ=0.154 18 nm, U=40 kV, I=40 mA) at 298 K. Thermo-gravimetry (TG) were carried out between 30 and 800 °C at a scan rate of 10 °C·min⁻¹ in a N₂ atmosphere on a TGA Mettler-Toledo GmbH thermo-

gravimetric analyzer. Micro-analysis service was recorded on a Heraeus CHN-O-Rapid. Fluorescent spectra were carried on a Hitachi F-4600 spectrophotometer.

1.2 Syntheses of compounds 1~3

1.2.1 Synthesis of (btzH)[PbCl₃] (**1**)

To a solution of PbCl₂ (0.20 g, 0.72 mmol) in concentrated HCl (18 mL, 47%) was added a solution of benzothiazole (0.20 g, 1.52 mmol) in concentrated HCl (18 mL, 47%). The mixed solution was heated to 80 °C and kept stirring for half hour. Cooling down the reaction to room temperature gave colorless needle crystals. Yield: 144 mg, 44% (based on PbI₂). Anal. Calcd. for C₇H₆NSCl₃Pb(%): C 18.69, H 1.34, N 3.11. Found (%): C 18.36, H 1.69, N 3.33. IR (KBr, cm⁻¹): 3 740(w), 3 440(s), 3 094(m), 3 046(w), 2 948(m), 2 865(m), 2 802(m), 2 742(m), 2 646(m), 1 852(m), 1 716(m), 1 596(m), 1 580(m), 1 458(m), 1 428(m), 1 271(m), 1 241(m), 952(s), 888(s), 800(w), 755(w), 721(m), 686(m), 554(w), 503(w), 423(w).

1.2.2 Synthesis of (btzH)₂[CdCl₄]·2H₂O (**2**)

According to the similar procedure to synthesis of compound **1** based on CdCl₂ (0.359 g, 1.96 mmol) and benzothiazole (0.396 g, 2.93 mmol) in concentrated HCl (18 mL, 47%) gave the light gray prismatic crystals of **2**. Yield: 124 mg, 72%. Anal. Calcd. for C₁₄H₁₆N₂O₂S₂Cl₄Cd(%): C 29.89, H 2.87, N 4.98. Found (%): C 29.64, H 2.43, N 4.72. IR (KBr, cm⁻¹): 3 424(s), 3 102(m), 3 052(w), 2 963(m), 2 895(m), 2 813(m), 2 745(m), 2 359(s), 1 811(w), 1 603(w), 1 579(s), 1 461(s), 1 429(m), 1 244(s), 825(s), 761(w), 722(s), 566(w), 504(w), 413(w).

1.2.3 Synthesis of (btzH)₂[CoCl₄]·2H₂O (**3**)

According to the similar procedures to synthesis of compound **1** based on CoCl₂·6H₂O (0.50 g, 1.83 mmol) and benzothiazole (0.49 g, 3.63 mmol) in concentrated HCl (18 mL, 47%) gave the deep blue block crystals of **3**. Yield: 400 mg, 43%. Anal. Calcd. for C₁₄H₁₆N₂O₂S₂Cl₄Co(%): C 33.03, H 3.17, N 5.50%. Found (%): C 33.47, H 3.31, N 5.13. IR (KBr, cm⁻¹): 3 738(w), 3 411(w), 3 076(w), 3 029(m), 2 946(m), 2 878(w), 2 809(w), 2 744(m), 2 658(m), 2 365(s), 1 833(w), 1 702(s), 1 626(s), 1 586(s), 1 460(m), 1 413

(m), 1 294(s), 1 266(s), 1 244(s), 1 168(s), 1 046(s), 912(m), 822(s), 757(w), 721(m), 685(s), 538(w), 497(w), 418(s).

1.3 X-ray crystallography

In the crystallographic data collection of compounds **1**~**3**, standard procedures were used for mounting the crystals on a Bruker SMART CCD diffractometer with graphite-monochromated Mo $K\alpha$ radiation ($\lambda=0.071\ 073\ \text{nm}$). The structures were solved by the direct methods routines in the SHELXS program and refined on F^2 in SHELXL^[31]. Non-hydrogen atoms

were first refined isotropically followed by anisotropic refinement by full matrix least-squares calculations based on F^2 using SHELXL-97^[32]. All hydrogen atoms except that in water molecules were placed in idealized positions and treated as riding atoms. Hydrogen atoms in water molecules were first located in the difference Fourier maps then positioned geometrically and allowed to ride on their respective parent atoms. Details of the data collection and refinement are given in Table 1.

CCDC: 1571943, **1**; 1571944, **2**; 1571945, **3**.

Table 1 Crystal data and structure refinement for compounds **1**~**3**

Compound	1	2	3
Formula	C ₇ H ₆ NSCl ₃ Pb	C ₁₄ H ₁₆ N ₂ O ₂ S ₂ Cl ₄ Cd	C ₁₄ H ₁₆ N ₂ O ₂ S ₂ Cl ₄ Co
Formula weight	449.75	562.64	509.16
Crystal system	Triclinic	Triclinic	Monoclinic
Space group	$P\bar{1}$	$P\bar{1}$	$C2/c$
a / nm	0.425 31(16)	0.740 78(5)	1.159 2(5)
b / nm	1.146 2(4)	0.772 47(5)	1.007 7(4)
c / nm	1.288 7(5)	1.890 52(11)	1.798 5(7)
$\alpha / (^\circ)$	64.830(7)	101.000 0(10)	90
$\beta / (^\circ)$	82.343(8)	96.678 0(10)	104.142(4)
$\gamma / (^\circ)$	84.459(8)	94.541 0(10)	90
V / nm^3	0.563 0(4)	1.049 02(12)	2.037 2(14)
Z	2	2	4
$D_c / (\text{g}\cdot\text{cm}^{-3})$	2.653	1.781	1.660
μ / mm^{-1}	15.833	1.760	1.583
$F(000)$	408	556	1 028
θ_{max}	25.00	36.57	27.88
Total reflection	3 382	12 228	7 893
Unique reflection	1 911 ($R_{\text{int}}=0.041\ 8$)	8 205 ($R_{\text{int}}=0.013\ 5$)	2 248 ($R_{\text{int}}=0.016\ 6$)
Completeness / %	97.0	99.3	98.6
No. of variables	123	250	127
GOF	1.090	1.072	1.041
$R_1, wR_2 [I>2\sigma(I)]$	0.033 3, 0.086 7	0.037 6, 0.084 4	0.022 9, 0.058 5
R_1, wR_2 (all data)	0.034 0, 0.087 5	0.048 7, 0.092 7	0.027 5, 0.061 1

2 Results and discussion

2.1 Synthesis and characterization

Compounds **1**~**3** were obtained by reactions of MX₂ (M=Pb, Cd, Co) and btz with molar ratio of 1:2 in concentrated HCl solution. After heating and evaporation, the reactions led to the formation of colorless needle crystals of **1**, light gray plate crystals

of **2** and deep blue block crystals of **3** in moderate yields, respectively. Crystals were then filtered and washed with methanol and acetonitrile and dried in vacuo. The phase purities of a mass of **1**~**3** were verified using the powder X-ray diffraction (PXRD) patterns which matched very well with the simulated ones in terms of the single-crystal X-ray data as shown in Fig.S1.

The TGA curves for compounds **1**~**3** were provided in Fig.S2. Complex **1** occurs two weight loss steps between 180 and 750 °C. The first weight loss, observed between 180 and 200 °C, is ascribed to the decomposition of the btz ligand (30% loss). The second weight loss, occurring between 550 to 750 °C, is attributed to the loss of halide anions or sublimation of newly formed PbCl₂ compound. While complex **2** is not stable, it firstly decomposes at 100 °C due to the loss of solvated water (6%). The second and third weight loss between 150 to 280 °C are ascribed to the loss of btz ligand (49%). The last weight loss began at 560 °C is corresponded to the loss of CdCl₂, which is consistent with its melting point at 568 °C. The residue (1.5%) may belong to the high boiling impurities. The weight loss of compound **3** is somewhat familiar to complex **2**, but the weight loss curve is not as clear as that in complex **2**.

In FT-IR spectra of compounds **1**~**3**, the strong absorption bands at 1 580 and 1 596 cm⁻¹ for **1**, 1 579 and 1 603 cm⁻¹ for **2**, 1 586 and 1 626 cm⁻¹ for **3** are ascribed to the C=C and C=N stretching vibrations of aromatic rings. The middle absorptions at 3 094, 3 046 cm⁻¹ for **1**, at 3 102, 3 052 cm⁻¹ for **2** and at 3 076, 3 029 cm⁻¹ for **3** are corresponded to the vibration of C-H bond in benzothiazole ring. The C-S stretching vibration in compounds **1**~**3** is about at 722 cm⁻¹. Due to the formation of hydrogen bond, the vibration of N-H in benzothiazole ring becomes very weak. The broad

and strong bands at about 3 400 cm⁻¹ in compounds **2** and **3** indicate the presence of co-crystallized water molecules.

2.2 Structure description

Complex **1** crystallizes in the triclinic system with a space group of $P\bar{1}$ and the asymmetric unit contains one (btzH)⁺ cation, one [PbCl₃]⁻ anion (Fig. 1a). Based on the connectivity of the chlorine atoms to the Pb atoms, there are three types of chlorine atoms: the terminal Cl(3), the double bridging Cl(1), and the triple-bridging Cl(2). The inorganic part of **1** is composed of [PbCl₆] octahedrons by sharing three edges along *a* axis direction to give 1D double-strand (Fig.1b). The protonated (btzH)⁺ cations are connected to the double-strands by intermolecular hydrogen bond N-H···Cl along *c* axis direction (Table 4). In [PbCl₆] octahedron, the Pb-Cl bond lengths vary from 0.275 6(2) to 0.304 3(2) nm, and the maximum angle of Cl-Pb-Cl is at 174.53(6)°, revealing the octahedron was seriously distorted (Table 2).

Complex **2** crystallizes in the triclinic system with a space group of $P\bar{1}$ and the asymmetric unit contains two protonated (btzH)⁺ cations, one [CdCl₄]²⁻ anion and two solvated water molecules (Fig.2a). The coordination geometry around the Cd(II) atom adopts a slightly distorted tetrahedron with the Cd-Cl bond lengths varying from 0.244 34(7) to 0.245 39(6) nm, and the angles varying from 105.89(4)° to 114.25(3)° (Table 3). In the whole structure, two water molecules

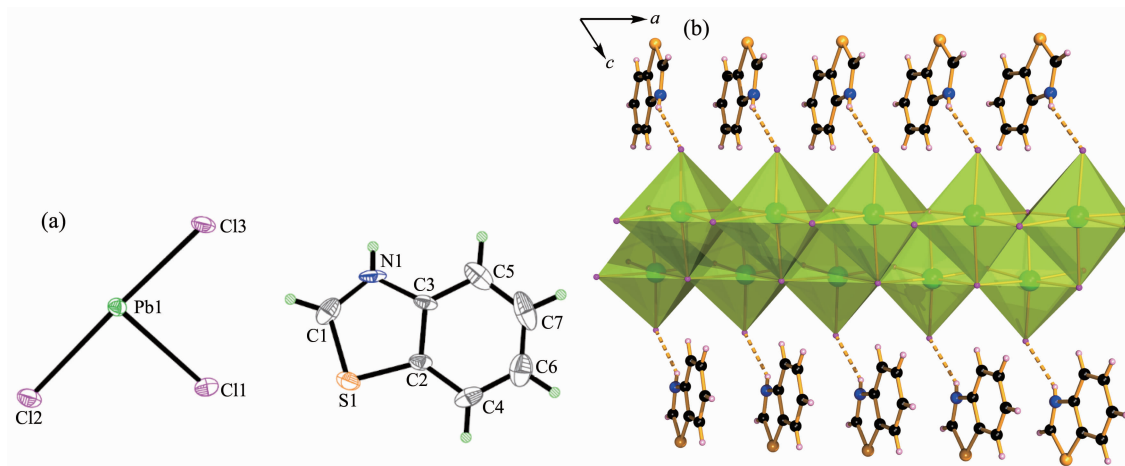


Fig.1 (a) Asymmetric unit of **1** drawn with 30% thermal ellipsoids; (b) Protonated (btzH)⁺ cations connected to 1D double-strands by N-H···Cl hydrogen bonds

Table 2 Selected bond lengths (nm) and angles (°) for **1**

Pb(1)-Cl(1)	0.279 9(2)	Pb(1)-Cl(2)	0.304 3(2)	Pb(1)-Cl(3)	0.275 6(2)
Pb(1)-Cl(2) ⁱ	0.289 1(3)	Pb(1)-Cl(1) ⁱⁱ	0.293 7(2)	Pb(1)-Cl(2) ⁱⁱⁱ	0.297 2(3)
Cl(2) ⁱ -Pb(1)-Cl(2)	81.50(7)	Cl(1) ⁱⁱ -Pb(1)-Cl(2) ⁱⁱⁱ	83.43(7)	Cl(2) ⁱⁱⁱ -Pb(1)-Cl(2)	83.76(7)
Cl(3)-Pb(1)-Cl(1)	86.63(7)	Cl(1)-Pb(1)-Cl(2) ⁱ	87.38(7)	Cl(1)-Pb(1)-Cl(2)	90.90(7)
Cl(3)-Pb(1)-Cl(1) ⁱⁱ	92.54(7)	Cl(1)-Pb(1)-Cl(2) ⁱⁱ	92.90(7)	Cl(2) ⁱ -Pb(1)-Cl(2) ⁱⁱⁱ	92.99(7)
Cl(3)-Pb(1)-Cl(2) ⁱ	93.16(7)	Cl(1)-Pb(1)-Cl(1) ⁱⁱ	95.69(7)	Cl(3)-Pb(1)-Cl(2) ⁱⁱⁱ	98.79(6)
Cl(1)-Pb(1)-Cl(2) ⁱⁱⁱ	174.53(6)	Cl(3)-Pb(1)-Cl(2)	174.23(6)		

Symmetry codes: ⁱ -x, -y+3, -z-1; ⁱⁱ x+1, y, z; ⁱⁱⁱ -x+1, -y+3, -z-1.

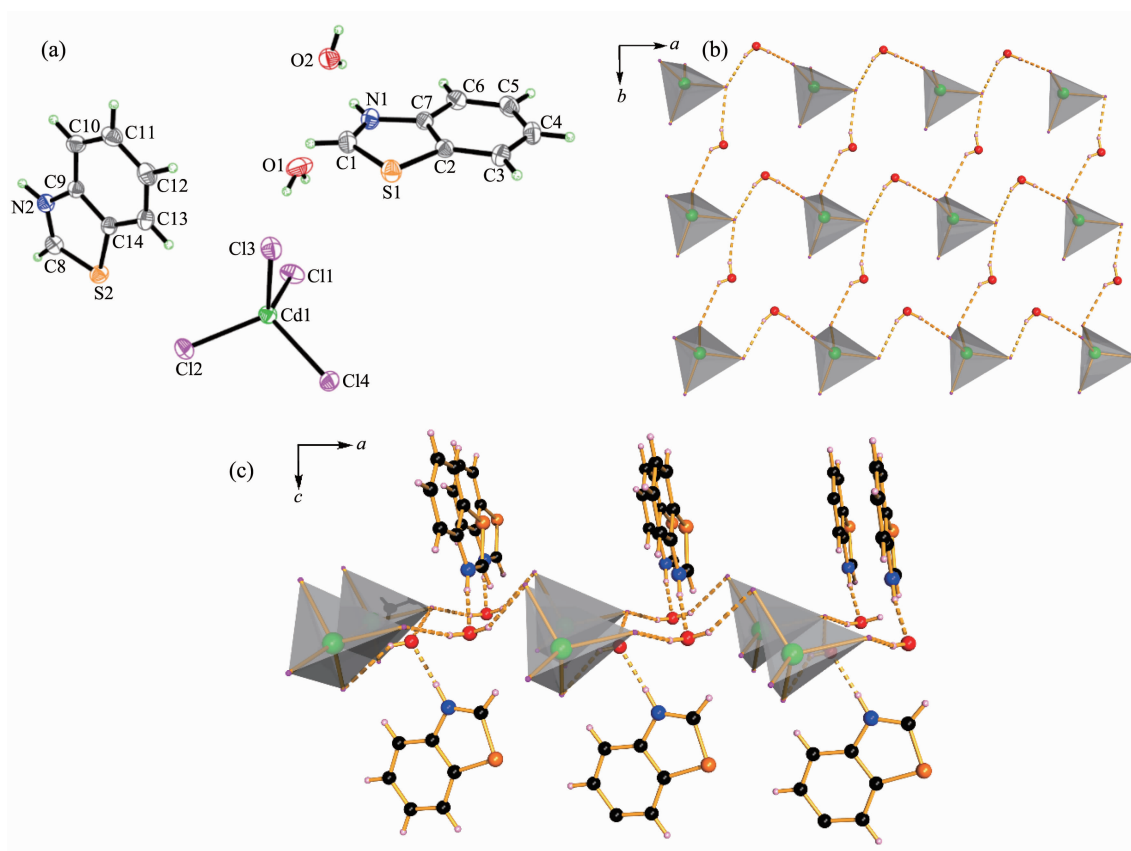


Fig.2 (a) Asymmetric unit of **2** drawn with 30% thermal ellipsoids; (b) $[\text{CdCl}_4]$ tetrahedrons connected with water molecules using hydrogen bonds $\text{O}-\text{H}\cdots\text{Cl}$ along a and b directions; (c) $(\text{btzH})^+$ cations connected to the 2D layers using hydrogen bond $\text{N}-\text{H}\cdots\text{O}$ along c direction

act as μ_2 -connecting nodes linking the $[\text{CdCl}_4]$ tetrahedrons by two pairs of hydrogen bonds ($\text{O}_{\text{water}}-\text{H}\cdots\text{Cl}$, Table 4) along a and b directions to form a 2D layer (Fig.2b). At the same time, the cationic $(\text{btzH})^+$ suspends on the 2D layer using the other type of hydrogen bond ($\text{N}-\text{H}\cdots\text{O}_{\text{water}}$) along c direction, (Table 4, Fig.3c).

Complex **3** crystallizes in the monoclinic system with a space group of $C2/c$ and the asymmetric unit

contains one protonated $(\text{btzH})^+$ cations, half $[\text{CoCl}_4]^{2-}$ anion and one solvated water molecules (Fig.3a). As shown in Fig.3b and 3c, the structure of compound **3** is very similar to that of complex **2**, so the structure of compound **3** is not described in detail herein. To be noted, the Co-Cl bond lengths in complex **3** are shorter than the Cd-Cl bond lengths in complex **2** due to that the radius of Co^{2+} ion is smaller than that of Cd^{2+} (Table 3). But the average bond angle Cl-Co-Cl

Table 3 Selected bond lengths (nm) and angles ($^{\circ}$) for **2** and **3**

2					
Cd(1)-Cl(1)	0.244 34(7)	Cd(1)-Cl(2)	0.245 07(7)	Cd(1)-Cl(3)	0.247 53(7)
Cd(1)-Cl(4)	0.245 39(6)				
Cl(1)-Cd(1)-Cl(2)	114.25(3)	Cl(1)-Cd(1)-Cl(4)	108.26(3)	Cl(2)-Cd(1)-Cl(4)	110.78(3)
Cl(1)-Cd(1)-Cl(3)	105.28(3)	Cl(2)-Cd(1)-Cl(3)	108.77(3)	Cl(4)-Cd(1)-Cl(3)	109.29(3)
3					
Co(1)-Cl(1)	0.227 75(7)	Co(1)-Cl(2)	0.226 04(7)		
Cl(2)-Co(1)-Cl(2) ⁱ	111.19(4)	Cl(2)-Co(1)-Cl(1)	109.91(3)	Cl(2) ⁱ -Co(1)-Cl(1)	108.87(3)
Cl(1)-Co(1)-Cl(1) ⁱ	108.03(4)				

Symmetry codes: ⁱ $-x+1, y, -z+1/2$ for complex **3**.

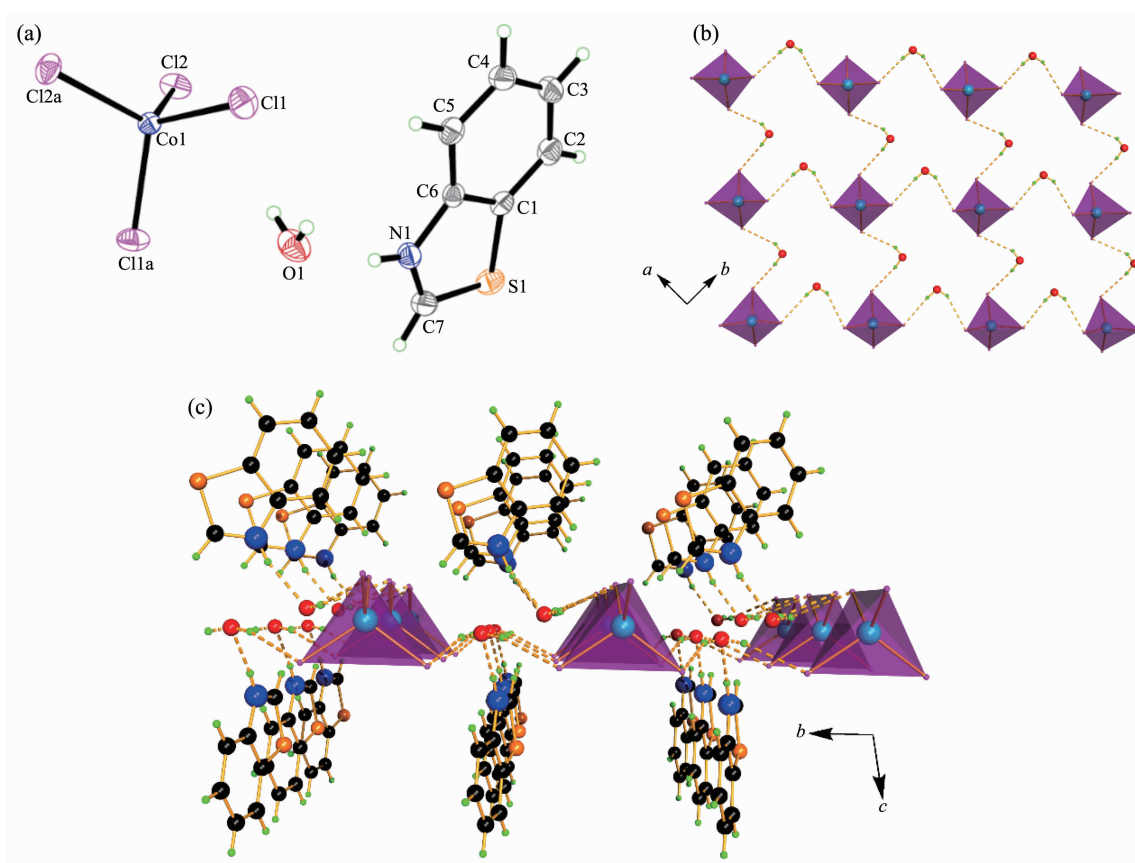


Fig.3 (a) Asymmetric unit of **3** drawn with 30% thermal ellipsoids; (b) [CoCl₄] tetrahedra connected by water molecules using hydrogen bonds O-H...Cl along *a* and *b* directions to form 2D layer; (c) (btzH)⁺ cations suspended on the 2D layers using hydrogen bond N-H...O_{water} along *c* direction

at 109.5 $^{\circ}$ in tetrahedron [CoCl₄] is similar to that of Cl-Cd-Cl (109.44 $^{\circ}$) in [CdCl₄].

2.3 Absorption and fluorescence

As shown in Fig.4, compounds **1**~**3** in the solid states showed the similar absorption wavelengths in

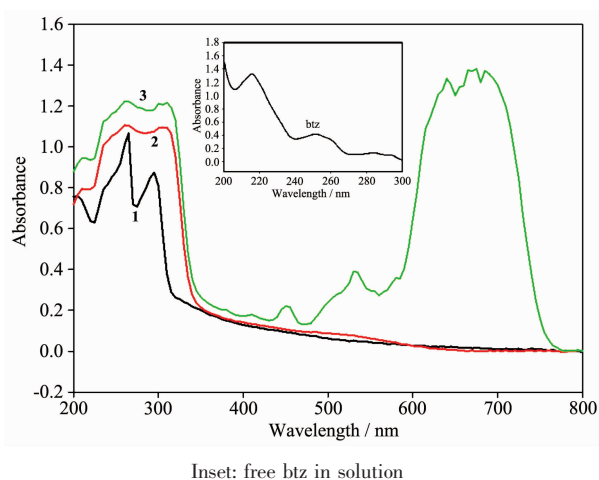
the range of 200~300 nm. The absorption peaks at 260 and 300 nm both come from the $\pi \cdots \pi^*$ transition of btz ring which can be proved by the absorptions of free ligand btz in solution (Fig.4, inset). Due to the strong absorption of organic part,

Table 4 Hydrogen bonds for compounds **1**, **2** and **3**

D-H...A	<i>d</i> (D-H) / nm	<i>d</i> (H...A) / nm	<i>d</i> (D...A) / nm	∠DHA / (°)
1				
N(1)-H(1)···Cl(3) ⁱ	0.076	0.245	0.310	145
2				
O(2)-H(W1)···Cl(3) ⁱⁱ	0.079(5)	0.242(5)	0.315 9(3)	155(5)
N(1)-H(1A)···O(2)	0.082(3)	0.190(3)	0.270 0(3)	168(3)
N(2)-H(2)···O(1) ⁱⁱⁱ	0.091(3)	0.180(3)	0.271 0(4)	176(3)
O(2)-H(W2)···Cl(4) ^{iv}	0.085(5)	0.241(5)	0.319 9(3)	156(5)
O(1)-H(W3)···Cl(3)	0.088(8)	0.248(8)	0.330 5(4)	157(6)
O(1)-H(W4)···Cl(2) ⁱⁱ	0.074(7)	0.280(6)	0.336 1(4)	135(6)
3				
N(1)-H(1)···O(1)	0.083 0	0.194 3	0.275 6	166.33
O(1)-H(1W)···Cl(2) ^v	0.076 7	0.252 7	0.320 5	148.32
O(1)-H(2W)···Cl(1)	0.080 0	0.243 3	0.321 3	165.47

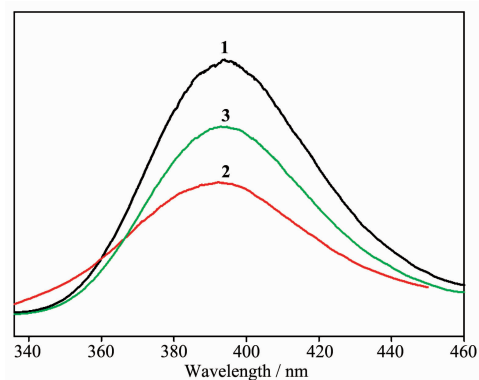
Symmetry codes: ⁱ $-x, 2-y, -z$ for **1**; ⁱⁱ $x, -1+y, z$; ⁱⁱⁱ $1-x, 1-y, 1-z$; ^{iv} $1+x, -1+y, z$ for **2**; ^v $1/2+x, 1/2+y, z$ for **3**.

the absorptions originated from inorganic parts [PbCl₆] in complex **1** and [CdCl₄] in complex **2** are not obvious. In **3**, the tetrahedrally coordinated Co²⁺ ions show the obvious absorption band in the range of 600~750 nm which belong to the spin allowed *d-d* transitions of Co²⁺ ion. While in complex **2**, the *d-d* transition is not found due to that the *d* orbits in Cd²⁺ ions are full.

Fig.4 UV-Vis spectra of compounds **1~3** in solid states

The solid fluorescent spectra of compounds **1~3** were showed in Fig.5. At the excitation wavelength of 320 nm, all compounds show the similar emissions at 393 nm. In order to clarify the fluorescence source of the compounds **1~3**, we carried out the fluorescence test of free ligand btz in solution, but it was found

that there was no fluorescence response in dichloromethane solution. According to the literatures, we know that benzothiazole has a large π -conjugated system, and many benzothiazole derivatives have exhibited good fluorescence properties^[33-35]. According to the above analysis, we still believe that the fluorescence emission peaks of compounds **1~3** are derived from the $\pi \cdots \pi$ transition of the btz ring. This is because the benzothiazole is protonated and hydrogen-bonded to the chloride atoms in polyhedron, and its fluorescence performance turns from original quenching into enhancement.

Fig.5 Emission spectra of compounds **1~3** in the solid states

3 Conclusions

Three organic-inorganic hybrid compounds were isolated by reactions of btz with MCl₂ (M=Pb²⁺, Cd²⁺,

Co²⁺) in concentrated HCl aqueous solution. The single X-ray diffraction investigation demonstrated that the inorganic part in complex **1** is a 1D two stranded chain, and those in compounds **2** and **3** are the [MCl₄] (M=Cd, Co) tetrahedrons, which are both linked with the solvated water molecules by the hydrogen bond. Fluorescent spectra reveal that compounds **1~3** show the similar emission peaks at 393 nm, which are ascribed to the $\pi \cdots \pi$ transition of the protonated btz ring.

Supporting information is available at <http://www.wjhxsb.cn>

References:

- [1] Bellettato M, Bonoldi L, Crucian G, et al. *J. Phy. Chem. C*, **2014**,**40**:7458-7467
- [2] Li D, Song J, Yin P, et al. *J. Am. Chem. Soc.*, **2011**,**40**:14010-14016
- [3] Li S Y, Liu Z H. *Inorg. Chim. Acta*, **2013**,**404**:219-223
- [4] Saparov B, Mitzi D B. *Chem. Rev.*, **2016**,**116**:4558-4596
- [5] Chen T Y, Shi L, Yang H, et al. *Inorg. Chem.*, **2016**,**55**:1230-1235
- [6] Fu Y, Lu H. *J. Mol. Struct.*, **2008**,**892**:205-209
- [7] Garcia-Fernandez A, Bermudez-Garcia J M, Castro-Garcia S, et al. *Inorg. Chem.*, **2017**,**56**:4918-4927
- [8] Zheng Y Y, Wu G, Deng M, et al. *Thin Solid Films*, **2006**,**514**:127-131
- [9] Ye H Y, Zhou Q, Niu X, et al. *J. Am. Chem. Soc.*, **2015**,**137**:13148-13154
- [10] Chen Z Y, Lin S, Huang Y L, et al. *J. Cluster Sci.*, **2017**,**28**:1551-1564
- [11] Guo H X, Li X Z, Huang S K, et al. *Inorg. Chem. Commun.*, **2010**,**13**:262-265
- [12] Hu M C, Wang Y, Zhai Q G, et al. *Inorg. Chem.*, **2009**,**48**:1449-1468
- [13] Li X M, Chen Y G, Su C, et al. *Inorg. Chem.*, **2013**,**52**:11422-11427
- [14] Luo Y, Gamliel S, Nijem S, et al. *Chem. Mater.*, **2016**,**28**:6536-6543
- [15] Liang R, Yan D, Tian R, et al. *Chem. Mater.*, **2014**,**26**:2595-2600
- [16] Fang Q R, Zhu G S, Shi X, et al. *J. Solid State Chem.*, **2004**,**177**:1060-1066
- [17] Li Y, Liu Y, Gong P, et al. *Inorg. Chem. Commun.*, **2016**,**74**:42-47
- [18] Mao C Y, Liao W Q, Wang Z X, et al. *Inorg. Chem.*, **2016**,**55**:7661-7666
- [19] Que C J, Mo C J, Li Z Q, et al. *Inorg. Chem.*, **2017**,**56**:2467-2472
- [20] Wu G, Cheng S, Deng M, et al. *Synth. Met.*, **2009**,**159**:2425-2429
- [21] Zhang S, Zhao J, Ma P, et al. *Cryst. Growth Des.*, **2012**,**12**:1263-1272
- [22] Cariati E, Lucenti E, Botta C, et al. *Coord. Chem. Rev.*, **2016**,**306**:566-614
- [23] Liu X J, Fang Q R, Zhu G S, et al. *Inorg. Chem. Commun.*, **2004**,**7**:31-34
- [24] Sun X F, Wang Z, Li P F, et al. *Inorg. Chem.*, **2017**,**56**:3506-3511
- [25] Mao L, Wu Y, Stoumpos C C, et al. *J. Am. Chem. Soc.*, **2017**,**139**:5210-5215
- [26] Wang M J, Chen X R, Tong Y B, et al. *Inorg. Chem.*, **2017**,**56**:9525-9534
- [27] Wu Z, Li L, Ji C, et al. *Inorg. Chem.*, **2017**,**56**:8776-8781
- [28] Parola S, Julian-Lopez B, Carlos L D, et al. *Adv. Funct. Mater.*, **2016**,**26**:6506-6544
- [29] Tan Z, Wu Y, Hong H, et al. *J. Am. Chem. Soc.*, **2016**,**138**:16612-16615
- [30] Yu H, Wei Z H, Hao Y H, et al. *New J. Chem.*, **2017**,**41**:9586-9589
- [31] Sheldrick G M. *SHELXS-97, Program for the Solution of Crystal Structures*, University of Göttingen, Germany, **1997**.
- [32] Sheldrick G M. *SHELXL-97, Program for Refinement of Crystal Structures*, University of Göttingen, Germany, **1997**.
- [33] Yao D, Zhao S, Guo J, et al. *J. Mater. Chem.*, **2011**,**21**:3568-3570
- [35] Wu Z, Wu X, Li Z, et al. *Bioorg. Med. Chem. Lett.*, **2013**,**23**:4354-4357
- [34] Liu S D, Zhang L W, Liu X. *New J. Chem.*, **2013**,**37**:821-826